Wang et al. Robotics and Biomimetics 2014, 1:18
http://www.jrobio.com/content/1/1/18

Robotics and Biomimetics
a SpringerOpen Journal

RESEARCH Open Access

Magnetic microrobot and its application in a microfluidic system

Jingyi Wang[1,2], Niandong Jiao[1*], Steve Tung[1,3] and Lianqing Liu[1*]

Abstract

This paper researches the design and control method of a microrobot in a microfluidic system by electromagnetic field. The microrobot can move along the microchannel to a required position, and by changing the magnetic torque, the microrobot can also rotate in the microfluidic chip. As an application of the microrobot, it is used as a mobile micromixer to mix two solutions in the microfluidic chip, and the experimental results verify its effectiveness.

Keywords: Microrobot; Magnetic drive; Microfluidic; Micromixer

Background

Microrobot is a hot research field in robotics. Using microrobots as a tool to surgery *in vivo* has the advantages of small trauma, safety, reliability, and significant reduction of medical costs and rehabilitation duration, so entering the liquid environment of the human body and making *in vivo* detection and treatment [1-3] are an important developing direction of microrobots. Recently, many researches on microrobots have carried out a lot of various actuation methods for microrobots, such as electromagnetic actuators [4,5], chemical bubble actuators [6,7], swimming tail actuators [8-10], bacterial actuators [11-13], and so on. Especially, the electromagnetic driving method has many advantages. First, electromagnetic field can be used to drive the microrobot with high controllability through changing the currents of the electromagnetic coils. Second, magnetic field will not cause harm or side effects to humans.

Among the researches of magnetic controlled microrobots, Bradley J. Nelson's group, inspired by the natural design of bacterial flagella, proposed an artificial bacterial flagella microrobot [14] that could swim in a controllable fashion using weak applied magnetic fields. The flagella microrobot consisted of a helical tail and a small soft magnetic material as a head on one end. The flagella microrobot's helical propulsion could be precisely controlled by electromagnetic coils. They also proposed porous microniches using 3D laser lithography as a transporting microrobot for targeted cell delivery [15]. Metin Sitti proposed a microrobot driven by magnetic torque. It could be controlled by two pairs of Helmholtz coils and a pair of clamping coils with a stick-slip motion [16]. The horizontal movement was controlled by the Helmholtz coils, and the clamping coils made the driving signals for the stick-slip motion. Sukho Park proposed a kind of microrobot controlled by magnetic force. The driving system consisted of two pairs of Helmholtz coils and two pairs of Maxwell coils [17]. The magnetic force was provided by the Maxwell coils, and the Helmholtz coils were used to generate the torque for the rotation of the microrobot. However, in manipulating microrobots to explore the human body, there are still a lot of works that need to be done.

In order to control the microrobot to fulfill a specific function in the internal liquid environment of the human body, it is necessary to firstly control the microrobot's movement in the microfluidic environment simulating the vessels. Since a microfluidic system has an effective functional zone of microscale as well as precise control of flow rate, it can well simulate the vessel liquid environment [18].

This paper researches the design and fabrication of a microrobot controlled by outside electromagnetic field and proposes a control method for the motion of the microrobot in the microfluidic system. This microrobot can move along the microchannel to a required position. By changing the magnetic torque, the microrobot can

* Correspondence: ndjiao@sia.cn; lqliu@sia.cn
[1]State Key Laboratory of Robotics, Shenyang Institute of Automation, Chinese Academy of Sciences, No.114 Nanta Street, Shenyang 110016, China
Full list of author information is available at the end of the article

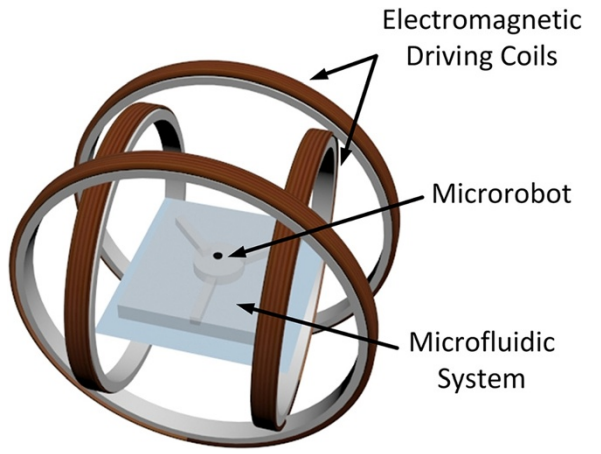

Figure 1 Magnetic driving system for the microrobot in a microfluidic system.

also rotate in the microfluidic chip. As an application of the microrobot, it can be used as a mobile micromixer in the microfluidic chip.

Methods

Theoretical model

In order to study the movement of the microrobot in a microfluidic system, the force acting on the microrobot and the action of the magnetic field are analyzed. The microrobot is designed to be a hemispherical structure and located in the magnetic driving system, which has four independent controlling electromagnetic coils. The system structure is shown in Figure 1. When the microrobot is suspended in the liquid, gravity is equal to buoyancy. So force analysis is mainly in the horizontal direction. When the microrobot is immersed in the liquid, magnetic force is the main driving force that works on the robot. And the viscous force has a relationship with the velocity of the microrobot:

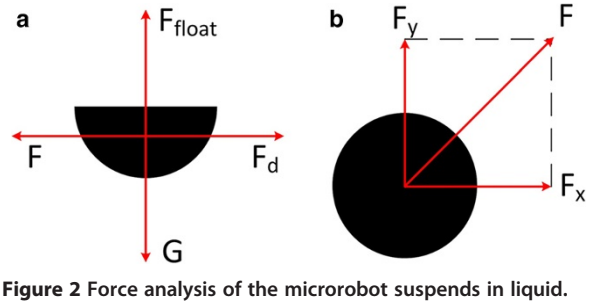

Figure 2 Force analysis of the microrobot suspends in liquid. **(a)** Side view of the microrobot. The forces acting on the microrobot in the horizontal direction are magnetic force and viscous force. In the vertical direction, buoyancy and gravity are equal when the microrobot is suspended in the channel. **(b)** Top view of the microrobot. Magnetic force can be decomposed into two components in the *x*, *y* direction.

$$F + F_d + m\frac{dv}{dt} = 0 \tag{1}$$

where v is the velocity of the microrobot. Force analysis of the microrobot immersed in liquid is shown in Figure 2.

In the horizontal direction, the resistance force works against the motion of the microrobot. In order to manipulate the microrobot, the input magnetic force must overcome the resistance:

$$F \geq F_d \tag{2}$$

where F is the magnetic force exerted on the microrobot and F_d is the resistance of the fluid. The magnetic force is given by:

$$F = V(M\cdot\nabla)B \tag{3}$$

where V is the volume of the magnetic microrobot, M is the uniform magnetization of the magnetic microrobot, and B is the magnetic flux. ∇ is the gradient operator:

$$\nabla = \begin{bmatrix} \frac{\partial}{\partial x} \\ \frac{\partial}{\partial y} \end{bmatrix} \tag{4}$$

$$M = \begin{bmatrix} M_x \\ M_y \end{bmatrix}, B = \begin{bmatrix} B_x \\ B_y \end{bmatrix} \tag{5}$$

Only considering in the xy plane, magnetic force can be expressed as the following vector form:

$$\begin{aligned} F = \begin{bmatrix} F_x \\ F_y \end{bmatrix} &= V \begin{bmatrix} \frac{\partial B_x}{\partial_x} & \frac{\partial B_y}{\partial_x} \\ \frac{\partial B_x}{\partial_y} & \frac{\partial B_y}{\partial_y} \end{bmatrix} \begin{bmatrix} M_x \\ M_y \end{bmatrix} \\ &= V \begin{bmatrix} M_x & \frac{\partial B_x}{\partial_x} \\ M_y & \frac{\partial B_y}{\partial_y} \end{bmatrix} \end{aligned} \tag{6}$$

The counter-diagonal of ∇B can be considered to be 0, and M_x and M_y are constants in the magnetic field simultaneously.

Therefore, the main factors of the direction and the force are $\frac{\partial B_x}{\partial x}$ and $\frac{\partial B_y}{\partial y}$. To generate the required gradient magnetic field, magnetic coils are needed. The magnetic field generated by the current flow through a circular electromagnetic coil can be calculated by the Biot-Savart law as follows:

$$B = \frac{\mu_0 I}{4\pi}\int_L \frac{dl \times r}{|r|^3} \tag{7}$$

where I is the current through the coil, L is the integral path, r is the full displacement vector from the wire

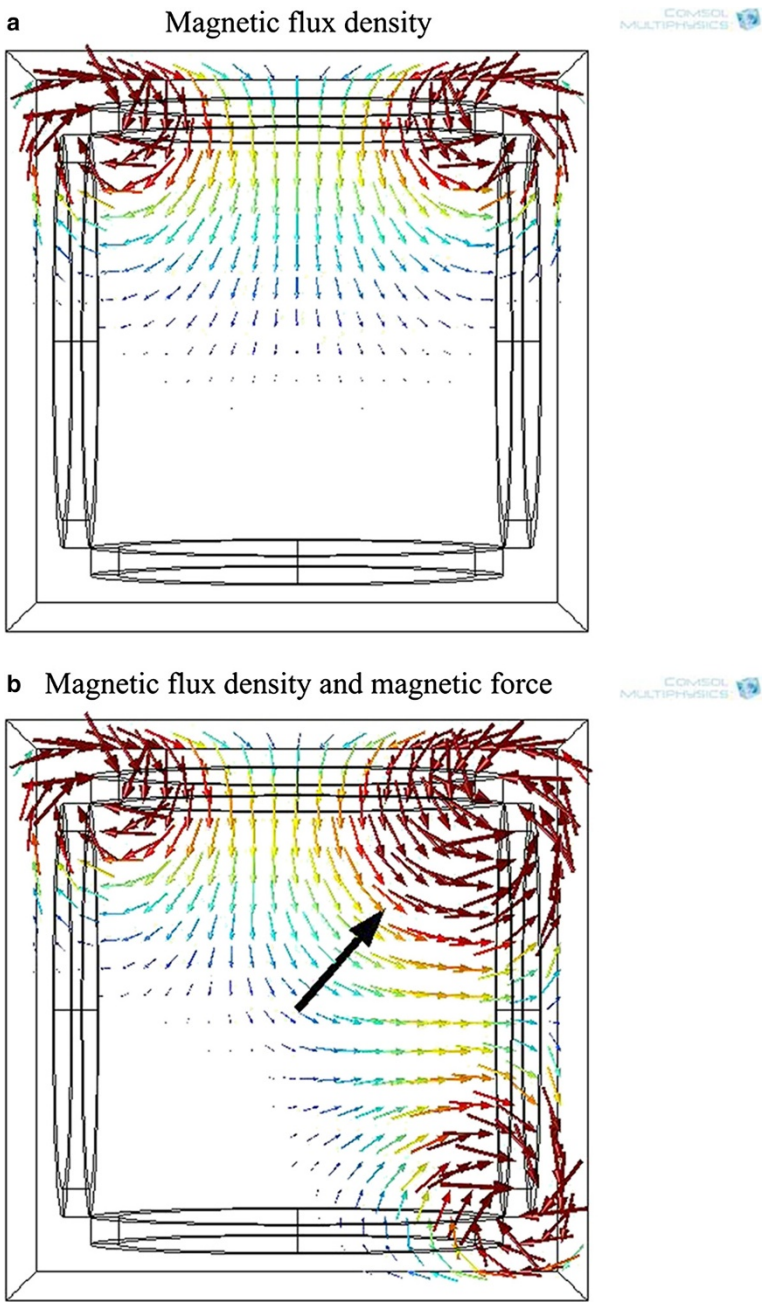

Figure 3 Simulation of the magnetic field generated in the *xy* plane. (a) Magnetic field generated by the top electromagnetic coil. **(b)** Magnetic field generated by the top and right electromagnetic coils. The black arrow indicates the resultant magnetic force generated by the two coils.

element to the point where the field needs to be calculated, dl is a vector of the differential element of the current through the wire, and μ_0 is the magnetic permeability ($\mu_0 = 4\pi \times 10^{-7}$ H/m).

To manipulate the microrobot accurately, the magnetic field produced by the electromagnetic coils must be controlled nicely. The microrobot is placed in the controlled area that is surrounded by four electromagnetic coils, and each electromagnetic coil can be controlled accurately according to the current outputting by the PC. Four coils can be controlled separately or together. COMSOL multiphysics is used to simulate the magnetic field and the force generated by the electromagnetic coils.

Figure 3 shows the simulation of the magnetic field generated by the electromagnetic coils in the *xy* plane. It is the top view of the four coils. Figure 3a shows the

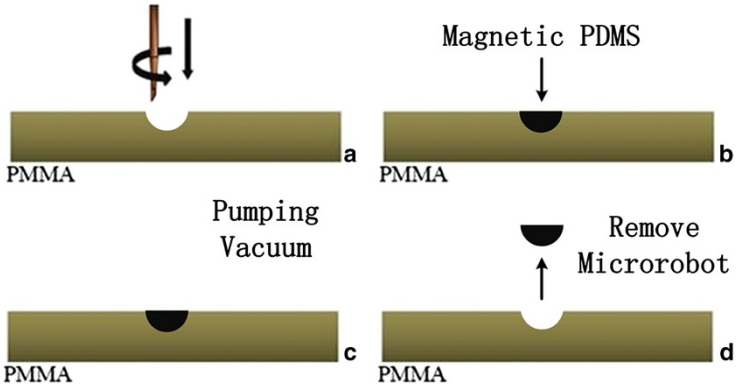

Figure 4 Process of microrobot fabrication. (a) Use an engraving machine curving the microrobot's mold. **(b)** Put the magnetic PDMS into the mold. **(c)** Degas and cure. **(d)** Remove the microrobot from the mold.

magnetic field generated by the top electromagnetic coil; the length and the direction of the arrow indicate the strength and the direction of the magnetic field, respectively. Figure 3b shows the magnetic field generated by the top and right electromagnetic coils; the black arrow indicates the resultant magnetic force generated by the top and right electromagnetic coils. By controlling the magnetic field, the strength and the direction of the resultant magnetic force can be regulated; therefore, the microrobot in the field can move freely in the plane.

Microrobot and system configuration

Fabrication of the microrobot

Polydimethylsiloxane (PDMS) has great plasticity and can be shaped to any structures depending on the needed size, shape, and so on. The microrobot is made of magnetic PDMS. To make magnetic PDMS, magnetic microparticles are added into PDMS. The microrobot is a hemispherical structure with a radius of 750 μm. Figure 4 shows the main production process of the microrobot:

1) Carve the microrobot's mold out of the acrylic plate using an engraving machine (Benchtop Engravers EGX-600/400, Roland DGA Corporation, Irvine, CA, USA) which is equipped with a milling cutter with a diameter of 200 μm.
2) Mix the polydimethylsiloxane and its curing agent at a mass ratio of 10:1 and then stir for 30 min.
3) Put NdFeB magnetic microparticles into mixed PDMS and then put them into the microrobot's mold.
4) Degas for 30 min in a vacuum box to remove bubbles.
5) Put the microrobot into an oven to heat for 3 h at 60°C.
6) Remove the microrobot from the mold with tweezers after magnetic PDMS is cured.

Setup of the magnetic driving system

The magnetic driving system consists of a PC, vision acquisition camera, data acquisition card (NI PCI-6229 DAQ Card, National Instruments, Austin, TX, USA), DC power supply, array of air-core electromagnetic coils, micron three-dimensional positioning stage, and power amplifier. The electromagnetic coils are supported on aluminous frames which will not affect the magnetic field by their nonmagnetic conductive property. The electromagnetic coils, the micron three-dimensional positioning stage, and the power amplifier are assembled on an aluminous platform with heat sinks. The schematic diagram of the platform is shown in Figure 5.

The detailed specification of the electromagnetic coils is described in Table 1. The picture of the whole magnetic driving system is shown in Figure 6.

The location information of the microrobot is acquired by the vision acquisition camera and sent to the PC. The

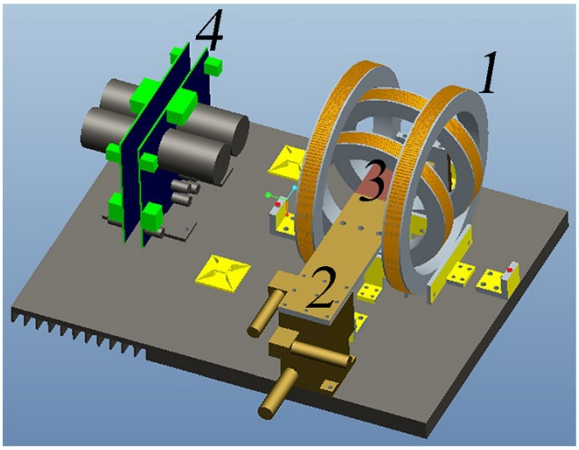

Figure 5 Schematic diagram of the magnetic driving platform. (1) An array of air-core electromagnetic coils. (2) A micron three-dimensional positioning stage. (3) Controlling area. (4) A power amplifier.

Table 1 Parameters of coils

Coils	Coil turns	Insider radius/outsider radius (mm)	Diameter of copper wires (mm)	Resistance (Ω)
x-axis	250	43.5/56.5	0.51	5
y-axis	250	62/75	0.51	6.5

control algorithm programmed by LabVIEW processes the location information and generates an output signal and then transmits it to the data acquisition card. The output signal is amplified through the power amplifier to generate the required magnetic field. When using the joystick to point a desired direction, the electromagnetic coils generate the needed magnetic force to control the microrobot. The microrobot in the microfluidic system is placed on the micron three-dimensional positioning stage in the center of the electromagnetic coils. The hardware connection of the magnetic driving system is shown in Figure 7.

Results and discussion

Motion control of the microrobot

To study the motion of the microrobot in the microfluidic channel, a microfluidic chip with cross-shaped channels is designed and fabricated. Potassium chloride solution is added into the microfluidic channels, so the microrobot can be suspended in the channel well. The solution in the microfluidic chip is in static state. The microfluidic chip is placed on the micron three-dimensional positioning stage and the positioning stage is adjusted so that the microfluidic chip is located in the magnetic driving system's controlling area. The width and depth of the microfluidic chip are both 3 mm. Figure 8 shows the motion of the microrobot in the microfluidic chip controlled by a joystick. The microrobot is located at the far left of the microfluidic chip. When using the joystick to control the microrobot to move to the center, the electromagnetic coil on the right generates the magnetic force. Then the microrobot is controlled to move to the top.

The microrobot starts to move in the channel due to the magnetic force. In the initial case, the magnetic force is greater than the liquid viscous force, with the increase of microrobot speed; fluid viscous force is gradually increased until the magnetic force is equal to the liquid viscous force. The microrobot reaches equilibrium.

The velocity of the microrobot is determined by the magnetic force, and the magnetic force can be changed by changing the currents in the electromagnetic coils. Figure 9 shows the velocities under different current values. With the increase of the current, the velocity of

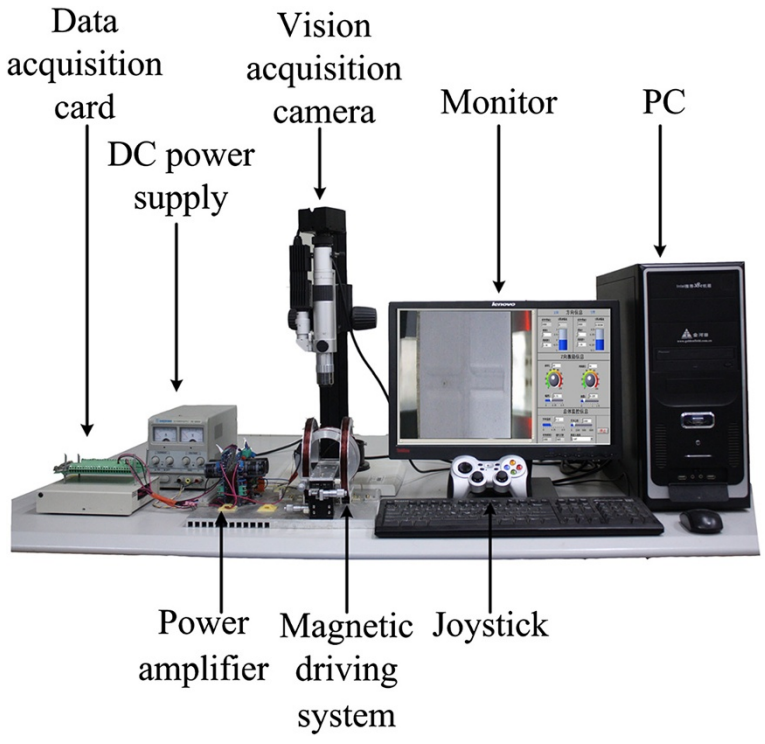

Figure 6 The whole magnetic driving system.

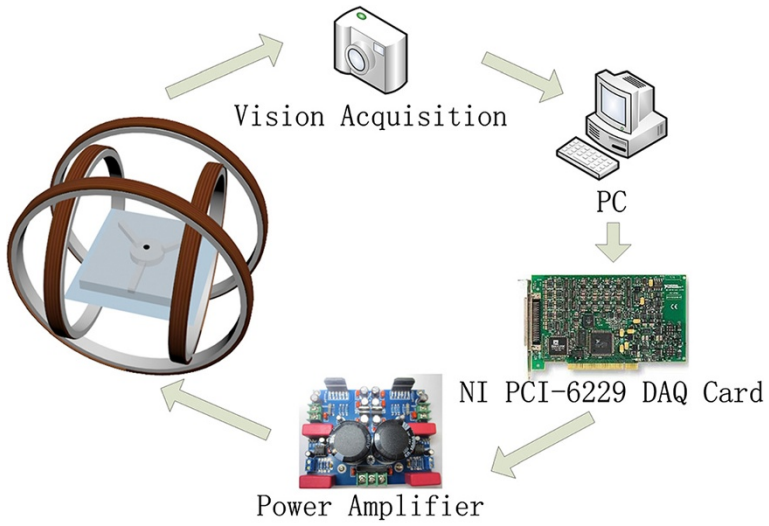

Figure 7 Hardware connection of the magnetic driving system.

the microrobot increases gradually, so the microrobot can be controlled precisely by changing the current.

The microrobot works as a mobile micromixer

The microrobot can move to any position in the microfluidic chip and can be controlled to produce rotary motion, so the microrobot can be used as a mobile micromixer in microfluidic chips.

In the existing micromixing research in microfluidics, two main kinds of micromixing technologies have been developed to improve mixing efficiency: passive and active micromixing. Passive micromixing generally has microchannels with complex design, special geometry [19], or additional complex obstacles [20] to increase contact with the liquid. Active micromixing mainly relies on the physical field that is exerted outside the microfluidic system. In accordance with the physical field exerted outside, the active micromixer is mainly divided into ultrasonic mixing [21], magnetic mixing [22,23], and so on. Active micromixing generally spends less time and has more simple structures. In this paper, a new mobile active micromixer has been proposed. A magnetic microrobot injected by a pipette into the microfluidic chip through the inlet can be controlled to move along the channel in a microfluidic chip, and when the desired location is reached, it can rotate to complete the mixing function as a mobile active micromixer. To prove that the microrobot can be used as a mobile micromixer, we fabricated a microfluidic chip and made a comparison by mixing two solutions with and without the magnetic mobile active micromixer. The microfluidic chip is a PDMS-glass chip that is used for mixing in the lab. The depth and radius of the mixing chamber are 1.2 and 3 mm,

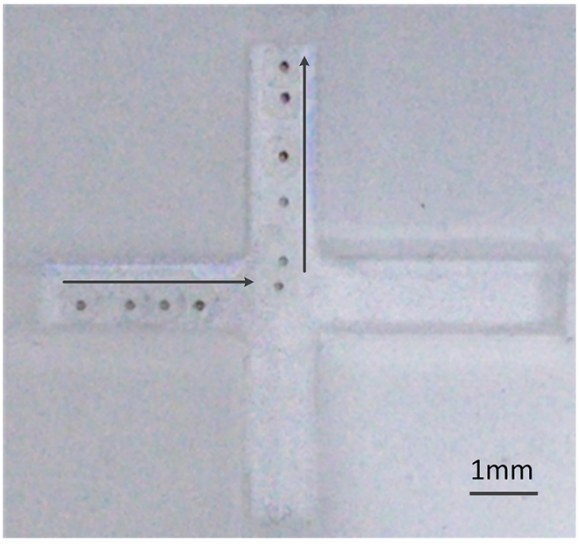

Figure 8 Motion of the microrobot in a fully static cross-shaped microfluidic channel. The width and depth of the microfluidic chip are both 3 mm. The microrobot is a hemispherical magnetic PDMS with a radius of 750 μm.

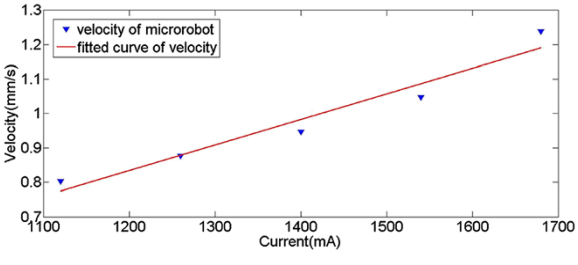

Figure 9 Velocity of the microrobot, along with the current in the electromagnetic coils. The red line indicates that the velocity increases with the current.

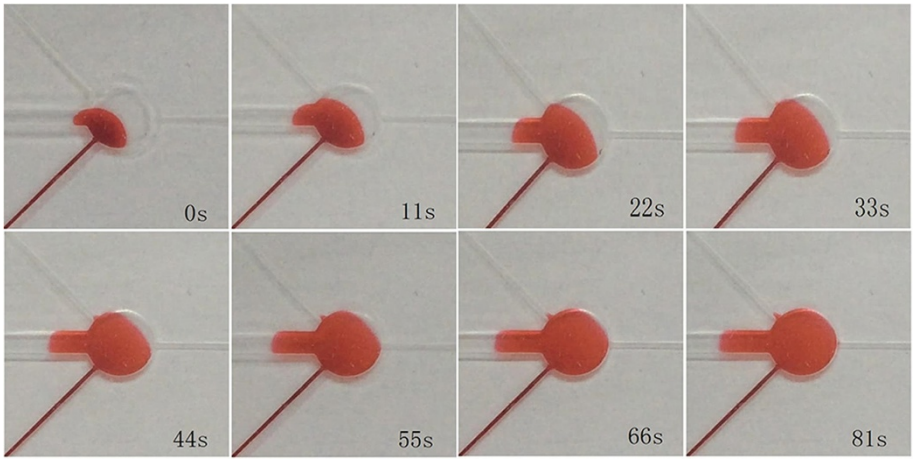

Figure 10 Natural mixing of potassium chloride solution and red pigment.

respectively. Colorless potassium chloride solution and red pigment were added into the mixing chamber for natural mixing, and the process was recorded by the vision acquisition camera. Figure 10 shows the process of natural mixing. Natural mixing mainly relies on the diffusion of liquid molecules. It takes 81 s until the diffusion is completed.

In the same condition with natural mixing, the microrobot moved through a microchannel (left side of the mixing chamber in Figure 11) into the mixing chamber of the microfluidic chip and then started to rotate clockwise with a frequency of 2 Hz to accelerate the mixing speed. Figure 11 shows the process of mixing with the microrobot. It takes only 32 s to complete the mixing.

The rotation made by the microrobot can generate significant tensile deformation and folding effect on the fluid streamline, so it increases the contact area between different liquids effectively. The rotational frequency of the microrobot can be increased by increasing the frequency of the sinusoidal signals provided in electromagnetic coils. To generate a rotating magnetic field, the sinusoidal signal is provided in each of the four coils, whose phase difference is 90°. When the rotational frequency increases, the microrobot can stir the liquid more quickly. Therefore, the microrobot can enhance the mixing efficiency with a larger rotational frequency. The microrobot can also move in the mixing chamber, and the motion can accelerate the mixing speed and enhance the mixing efficiency.

Conclusions

This paper researches the design and control method of a microrobot in microfluidics. A theoretical analysis is performed for the microrobot and magnetic driving system. The microrobot is made of magnetic PDMS. With four electromagnetic coils and other attachments, the magnetic driving system is constructed. By controlling the coils, the microrobot can move and rotate in a microfluidic chip. The

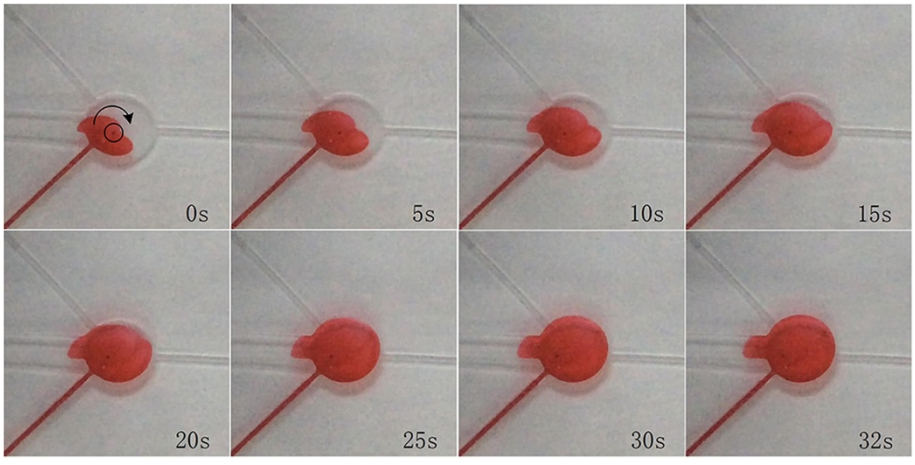

Figure 11 Process of the microrobot's mixing in the mixing chamber. The microrobot rotated clockwise with a frequency of 2 Hz. The black circle indicates the position of the microrobot, and the arrow shows the direction of the rotation.

microrobot can be used as a mobile micromixer, and a mixing experiment is accomplished inside a microfluidic mixing chip, which verifies the microrobot's effectiveness. Future studies will focus on the motion control of the microrobot in 3D and its interaction with live cells in a vessel-like microfluidic system.

Competing interests
The authors declare that they have no competing interests.

Authors' contributions
JW and NJ participated in the setup of the magnetic driving system and drafted the manuscript. JW carried out the analysis of the system and performed the experiments. ST provided advices and made contributions to the revision of the draft. LL proposed the basic idea and supervised the project. All authors read and approved the final manuscript.

Acknowledgements
This paper is supported by the National Natural Science Foundation of China (Grant Nos. 61106109 and 61304251) and the CAS FEA International Partnership Program for Creative Research Teams.

Author details
[1]State Key Laboratory of Robotics, Shenyang Institute of Automation, Chinese Academy of Sciences, No.114 Nanta Street, Shenyang 110016, China. [2]University of Chinese Academy of Sciences, No.19A Yuquan Road, Beijing 100049, China. [3]Department of Mechanical Engineering, University of Arkansas, W Dickson Street, Fayetteville, AR 72701, USA.

Received: 16 July 2014 Accepted: 16 October 2014
Published: 22 December 2014

References
1. Dario P, Hannaford B, Menciassi A (2003) Smart surgical tools and augmenting devices. Robot Autom IEEE Trans 19(5):782–792
2. Ponsky JL (2006) Endoluminal surgery: past, present and future. Surg Endosc Intervent Tech 20(2):S500–S502
3. Cuschieri A, Melzer A (1997) The impact of technologies on minimally invasive therapy. Surg Endosc 11(2):91–92
4. Xuanying L, Zhenbo L, Ling M, Dawei Z, Xiaoning T, Jiapin C (2013) Manufacturing and Wireless Driving of a Permanent Magnetic Micro-robot. Robot 35(5):513–520
5. Vollmers K, Frutiger DR, Kratochvil BE, Nelson BJ (2008) Wireless resonant magnetic microactuator for untethered mobile microrobots. Appl Phys Lett 92(14):144103
6. Sul OJ, Falvo MR, Taylor RM II, Washburn S, Superfine R (2006) Thermally actuated untethered impact-driven locomotive microdevices. Appl Phys Lett 89(20):203512
7. Búzás A, Kelemen L, Mathesz A, Oroszi L, Vizsnyiczai G, Vicsek T, Ormos P (2012) Light sailboats: laser driven autonomous microrobots. Appl Phys Lett 101(4):041111
8. Solovev AA, Mei Y, Bermúdez Ureña E, Huang G, Schmidt OG (2009) Catalytic microtubular jet engines self-propelled by accumulated gas bubbles. Small 5(14):1688–1692
9. Hwang G, Braive R, Couraud L, Cavanna A, Abdelkarim O, Robert-Philip I, Régnier S (2011) Electro-osmotic propulsion of helical nanobelt swimmers. Int J Robot Res 30(7):806–819
10. Edd J, Payen S, Rubinsky B, Stoller ML, Sitti M (2003) Biomimetic propulsion for a swimming surgical micro-robot. In: Proceedings of the IEEE/RSJ international conference on intelligent robots and systems, Las Vegas, 2003 (IROS 2003), vol 3., pp 2583–2588
11. Yamazaki A, Sendoh M, Ishiyama K, Ichi Arai K, Kato R, Nakano M, Fukunaga H (2004) Wireless micro swimming machine with magnetic thin film. J Magn Magn Mater 272:E1741–E1742
12. Dreyfus R, Baudry J, Roper ML, Fermigier M, Stone HA, Bibette J (2005) Microscopic artificial swimmers. Nature 437(7060):862–865
13. Darnton N, Turner L, Breuer K, Berg HC (2004) Moving fluid with bacterial carpets. Biophys J 86(3):1863–1870
14. Yesin KB, Vollmers K, Nelson BJ (2006) Modeling and control of untethered biomicrorobots in a fluidic environment using electromagnetic fields. Int J Robot Res 25(5–6):527–536
15. Kim S, Qiu F, Kim S, Ghanbari A, Moon C, Zhang L, Choi H (2013) Fabrication and characterization of magnetic microrobots for three-dimensional cell culture and targeted transportation. Adv Mater 25(41):5863–5868
16. Pawashe C, Floyd S, Sitti M (2009) Modeling and experimental characterization of an untethered magnetic micro-robot. Int J Robot Res 28(8):1077–1094
17. Choi J, Choi H, Jeong S, Park B, Ko S, Park J, Park S (2013) Position-based compensation of electromagnetic fields interference for electromagnetic locomotive microrobot. Proceedings of the Institution of Mechanical Engineers, Part C: Journal of Mechanical Engineering Science 227(9):1915–1926
18. Yeom E, Kang YJ, Lee SJ (2014) Changes in velocity profile according to blood viscosity in a microchannel. Biomicrofluidics 8(3):034110
19. Tran-Minh N, Frank K, Tao D (2014) A simple and low cost micromixer for laminar blood mixing: design, optimization, and analysis. Biomed Informat Technol 404:91–104
20. Murakami Y (2014) Mems mixer as an example of a novel construction method of microfluidics by discrete microparts. Sensors and Actuators B: Chemical 194:528–533
21. Yaralioglu GG, Wygant IO, Marentis TC, Khuri-Yakub BT (2004) Ultrasonic mixing in microfluidic channels using integrated transducers. Anal Chem 76(13):3694–3698
22. Lu LH, Ryu KS, Liu C (2002) A magnetic microstirrer and array for microfluidic mixing. Microelectromechanical Syst J 11(5):462–469
23. Wang Y, Zhe J, Chung BT, Dutta P (2008) A rapid magnetic particle driven micromixer. Microfluid Nanofluid 4(5):375–389

doi:10.1186/s40638-014-0018-z
Cite this article as: Wang *et al.*: **Magnetic microrobot and its application in a microfluidic system.** *Robotics and Biomimetics* 2014 **1**:18.